

Short Communication

Electrochromic and Electrochemical Energy Storage Properties of Micro-nano Hierarchical NiO film

YuJiang Zhu, YunHui Tang*, KaiLing Zhou, QianQian Zhang*, JingBing Liu, Hao Wang, and Hui Yan

Key Laboratory for New Functional Materials of Ministry of Education, College of Materials Science and Engineering, Beijing University of Technology, Beijing 100124, China.

*E-mail: tangyh@bjut.edu.cn, zhangqianqian@bjut.edu.cn

Received: 11 March 2019 / Accepted: 28 May 2019 / Published: 30 June 2019

Micro-nano hierarchical metal oxides offer unique advantages over traditional compact ones when serving as electrode materials, mainly because their good electrolyte wettability and high specific surface area can facilitate fast ion and electron transfer. Herein, we develop a facile route to fabricate micro-nano hierarchical NiO films for achieving enhanced bifunction of electrochromism and energy storage. The introducing of hierarchical structure effectively reduced the ion diffusion resistance and electron transfer resistance. As a result, hierarchical NiO films demonstrate superior electrochromic optical modulation and electrochemical energy storage compared with the compact ones. The transmittance change between the coloration and bleached states reaches 64.5% at 550 nm. Furthermore, the capacitance of hierarchical NiO is 14.85 F g⁻¹ at 0.2 mA cm⁻², which is approximately 20% higher than that of the compact NiO (12.36 F g⁻¹). This work provides an efficient way to prepare high-performance hierarchical NiO films, which can be extended to the fabrication of other metal oxides for wide applications in the highly efficient electrochemical utilization.

Keywords: hierarchical structure, NiO, electrochromic property, energy storage

1. INTRODUCTION

With the development of electrochemical energy storage devices, one of the greatest challenges is to enhance the efficiency of energy storage and conversion. In recent years, intense strategies have been proposed to boost the electrochemical utilization of electrode active materials, such as optimizing components [1-3] and designing structure [4-5]. In terms of structure design, controlling of size and shape of active materials could enhance the electrochemical performance when used as electrode materials [5-6]. Typical examples involve the construction of micro-nano hierarchical structure, which has attracted much attention in developing active electrode materials for electrochemical energy storage and conversion [7-9]. Usually, outer part of the active materials delivers more efficient redox reaction

compared with the inner one [10]. In this case, the loose and rough structure of micro-nano hierarchical films possess high specific surface area, which provide more active sites for highly effective electrode reactions. More importantly, as a well-known lotus-like structure, the micro-nano hierarchical film demonstrate both coarse and fine roughness [11]. According to the Wenzel equation [12-13], the electrolyte wettability of the electrode materials can be improved by introducing micro-nano hierarchical structure. This facilitate fast ion transfer between electrolyte and electrodes, which further enhance the electrochemical performance of the active materials.

Transition metal oxides is considered as a sort of classical electrode active materials owing to their good electrical conductivity and redox activity [14]. Among them, NiO is a typical example of active materials that exhibit not only electrochemical energy storage but also electrochromic behavior. During the charge/discharge process, NiO film demonstrate a reversible chromatic transition because of a change in the valence state driven by the redox reaction [15-17]. This bifunction have attract some research interest due to its potential applications in smart window and visual supercapacitors [18]. To achieve the bifunction, NiO film is usually much thinner than that used as pure electrode material due to the requirement of high transmittance [19-22]. It puts forward higher demand on the electrochemical utilization efficiency. In this paper, we present an improvement of bifunctional electrochromism and energy storage for NiO film by creating a micro-nano hierarchical structure. Compared with traditional compact NiO film, the hierarchical film exhibits a much higher transmittance modulation up to 64.5% (at 550 nm) when used as an electrochromic electrode. Furthermore, the capacitance of NiO obtained a 20% enhancement when introducing a hierarchical structure. This improvement in the electrochemical performance is ascribed to the increased electrolyte wettability and specific surface area, which contributed to fast ion and electron transfer in the electrolyte and active materials

2. EXPERIMENTAL

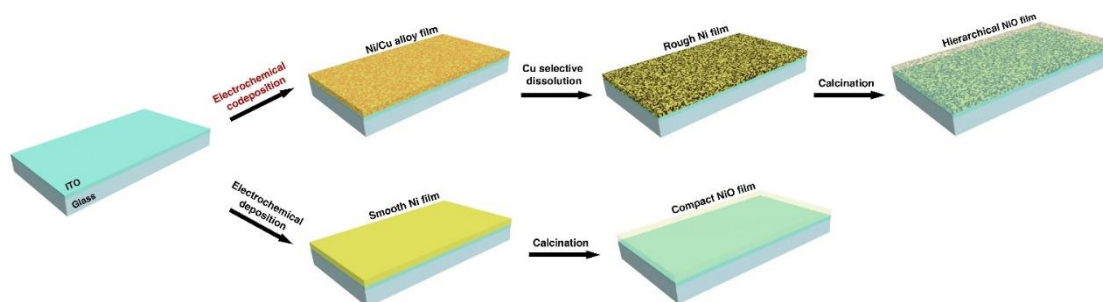
2.1. Materials

Anhydrous ethyl alcohol (C_2H_5OH), acetone, H_2SO_4 , $NiSO_4$ and $CuSO_4$ were purchased from Sinopharm Chemical Reagent Beijing Co., Ltd. $Na_3C_6H_5O_7$ and KOH were purchased from Tianjin Fuchen Chemical Regents Factory. And all reagents were used without further purification. The indium-tin oxide (ITO) glasses (Shenzhen South China Xiangcheng Technology Co., Ltd, $R_{\square} = 22 \Omega \square^{-1}$) were served as the optically transparent conductive substrates. In the electrochemical test, electrodes were bought from Tian Jin AIDAhengshneg Science-Technology Development Co., ltd.

2.2. Sample preparation

The process of sample preparation is shown in Scheme 1. The ITO glass was chosen as the substrate to fabricate hierarchical and compact NiO electrodes. Ni/Cu alloy coatings were firstly electrochemically deposited on the ITO glass (10 mm×20 mm) using the cyclic voltammetry (CV) method. During the codeposition, a linear-sweep potential between -1.0 V and 0.4 V was applied by a

CHI660E electrochemical workstation (Shanghai Chenhua Apparatus Co., China) at a scan rate of 0.01 V s^{-1} for 3 cycles. A platinum electrode and an Ag/AgCl electrode (in 3.5 mol L^{-1} KCl solution) served as the counter and reference electrodes, respectively. The electrolyte was an acidic aqueous solution (pH 4.0) containing 0.05 M CuSO_4 , 0.5 M NiSO_4 and $0.26 \text{ M Na}_3\text{C}_6\text{H}_5\text{O}_7$. The pH values of all electrolyte were adjusted by H_2SO_4 . Next, Cu was removed from the Ni/Cu alloy by a selective electrochemical dissolution at a constant anodic potential of 0.342 V for 200 s in above electrolyte. This produced a rough Ni film. For a control experiment, a smooth Ni film was directly deposited on the ITO glass using previously mentioned method in above electrolyte removing CuSO_4 . Finally, two kinds of Ni films were annealed at $300 \text{ }^\circ\text{C}$ under air ambient for an hour to induce hierarchical and compact NiO films formation.



Scheme 1. The fabrication process of hierarchical and compact NiO films on the ITO glass substrates.

2.3. Characterization

The surface morphologies of the samples in each step were observed by a Hitachi S4800 field emission Scanning electron microscopy (SEM). The X-ray photoelectron spectroscopy (XPS) spectra (Thermo escalab 250XI X-ray Photoelectron Spectroscopy) was used to determine the composition of samples. Water contact angle measurements were performed using a contact-angle system (GS Contact Angle Measuring Equipment, SufaceTech Co., LTD.) at ambient temperature and ca. 30% humidity.

2.4. Optical and Electrochemical Measurements

An ultraviolet–visible–near-infrared spectrophotometer (PERSEE TU-1810 PC) was employed to measure and record the transmission spectra of the NiO films in both fully colored and bleached states at the wavelength ranging from 300 nm to 800 nm . Moreover, electrochemical measurements were performed in a three-electrode system using a Princeton VersaSTAT 4 electrochemical workstation. Films have been cycled from -0.4 V to 0.6 V at a sweep rate of 0.05 V s^{-1} in 0.1 M KOH solution. During the measurements, the NiO films were acted as the working electrode, a Pt foil served as the counter electrode, and an Ag/AgCl (in 3.5 mol L^{-1} KCl solution) electrode was acted as the reference, respectively.

3. RESULTS AND DISCUSSION

Ni/Cu alloy film was firstly deposited on the ITO glass using the electrochemical codeposition method to fabricate the hierarchical NiO. Then, a rough Ni film was obtained after removing Cu from the alloy film. The as-prepared Ni film consisted of flower-like particles whose size ranging from several hundred nanometers to several micrometers (Figure 1a). In spite of a Ni metal film, the X-ray photoelectron spectroscopy (XPS) analysis also demonstrated the characteristic peaks of Ni²⁺, which may be ascribed to the oxidation of surface Ni and the contamination of Ni²⁺ ions from the electrolyte (Figure 1d). Finally, the rough Ni film was annealed in the air to induce NiO formation. As shown in Figure 2b, the carved flower-like Ni particles changed into larger rough particulates after calcination. The disappearance of Ni peak at 850 eV indicated the full oxidation of Ni film (Figure 1e). It is interesting that the obtained NiO particle exhibited a micro-nano hierarchical structure. The large microparticle was composed of many small nanoparticles. This hierarchical structure is the basis for acquiring super-lyophilic performance [23]. As a control, a smooth Ni film was electrochemically deposited on the ITO glass using the same fabrication parameters in the absence of Cu. The following calcination produced a flat and compact NiO film composed of uniform nanoparticles (Figure 1c). The above smooth and compact structure was not beneficial for the full oxidation of Ni, which reflected from the existence of the characteristic peaks of Ni metal in compact NiO film (Figure 1e). Therefore, the approach to obtain hierarchical NiO film could provide an effective path to achieve high electrochemical performance [17,18,24].

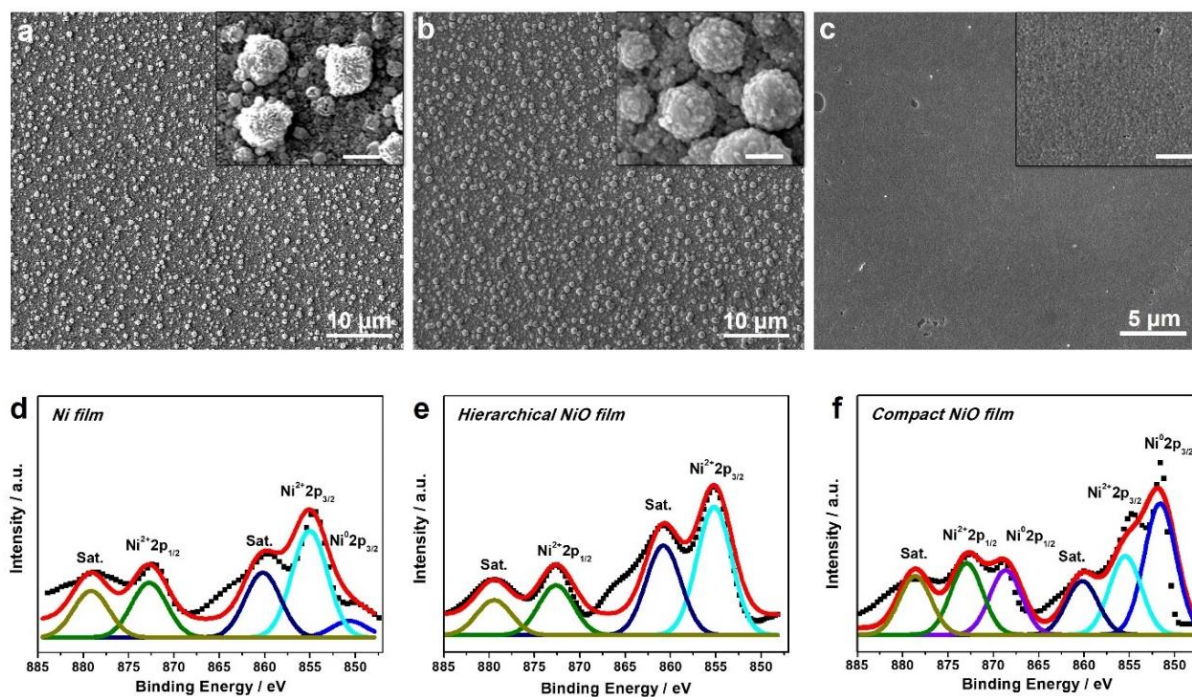


Figure 1. Top-view SEM images and corresponding XPS spectra of Ni film obtained after the dissolution of Cu from Ni/Cu alloy film (a, d), hierarchical NiO film (b, e) and compact NiO film (c, f). Insets in the SEM images are the magnified morphologies, and the scale bars are 1 μm.

To study the electrochemical properties of above hierarchical and compact NiO films, the cyclic voltammetry (CV) measurements were performed at a scan rate of 0.05 V s^{-1} in 1.0 mol L^{-1} KOH solution. Figure 2a show typical oxidation and reduction peaks of NiO, referring to the transformation between Ni^{2+} and Ni^{3+} because of double injection and extraction of ions (OH^- ions in this work) and electrons Equation (1) [25-28].



The area of closed CV curve for hierarchical NiO was much larger than that of the compact one, indicating that a higher charge storage capacity could be obtained when introducing a micro-nano hierarchical structure. As a well-known electrochromic material, NiO featured reversible chromatic transitions during the redox process [29]. The NiO film gradually turned to dark brown with being oxidized, while the reduction process drove the film to transparent (Equation 1) [30]. Comparing with compact NiO film, the hierarchical one demonstrated a much higher transparenance at the bleached state (-0.4 V) while a lower transparenance at the colored state ($+0.6 \text{ V}$) in the wavelength ranging from 300 to 800 nm (Figure 2b), owing to their distinct charge storage capacity. The difference in transmittance between colored and bleached states of hierarchical NiO film reached 64.5% at 550 nm (a wavelength most sensitive to the human eye), which was much higher than the compact one. And this data is also better than the previous work, whose optical modulation was 62% [8]. Therefore, the construction of micro-nano hierarchical structure could effectively enhance the optical modulation performance of the NiO film. The capacitive behaviors of the two NiO film were further evaluated through the galvanostatic charge/discharge measurements at various current densities. As shown in Figure 2c and 2d, the curve profile of the hierarchical NiO was symmetric and much prolonged over the compact NiO. Furthermore, hierarchical NiO embedded electrode exhibited a longer charge-discharge platform compared with the compact one, suggesting a more adequate redox reaction. According to the charge/discharge curve, the capacitance of the hierarchical NiO was determined to be 14.85 F g^{-1} at 0.2 mA cm^{-2} , which was approximately a 1.2-fold enhancement compared with the compact NiO (12.36 F g^{-1}). Meanwhile, the former literature had announced that the capacitance was about 12 F g^{-1} [18]. Hence, the introduction of micro-nano hierarchical structure contributed to a superior electrochemical energy storage behavior [31].

Table 1. Comparison in optical modulation and capacitance of hierarchical NiO film, compact NiO film and previous research in hierarchical NiO film.

	Optical Modulation (550 nm) %	Capacitance F g^{-1}
Hierarchical NiO	64.5	14.85
Compact NiO	4.2	12.36
Previous Research in Hierarchical NiO [18]	62	12

Finally, electrochemical impedance spectroscopy (EIS) were investigated to clarify the mechanism for enhanced bifunctional behaviors. The EIS measurements were performed at the frequency from 0.01 to 100000 Hz. In low frequency region, the Nyquist curve of hierarchical NiO

exhibited a much smaller slope than the compact one (Figure 3a), indicating an effective decrease in the ion diffusion resistance [32]. Furthermore, the hierarchical structure significantly increased the specific surface area of NiO film, which provided more active sites for effective electrochemical reaction [33]. This resulted in a decreased charge transfer resistance reflecting from a smaller radius of semicircle in high frequency region shown in Figure 3b.

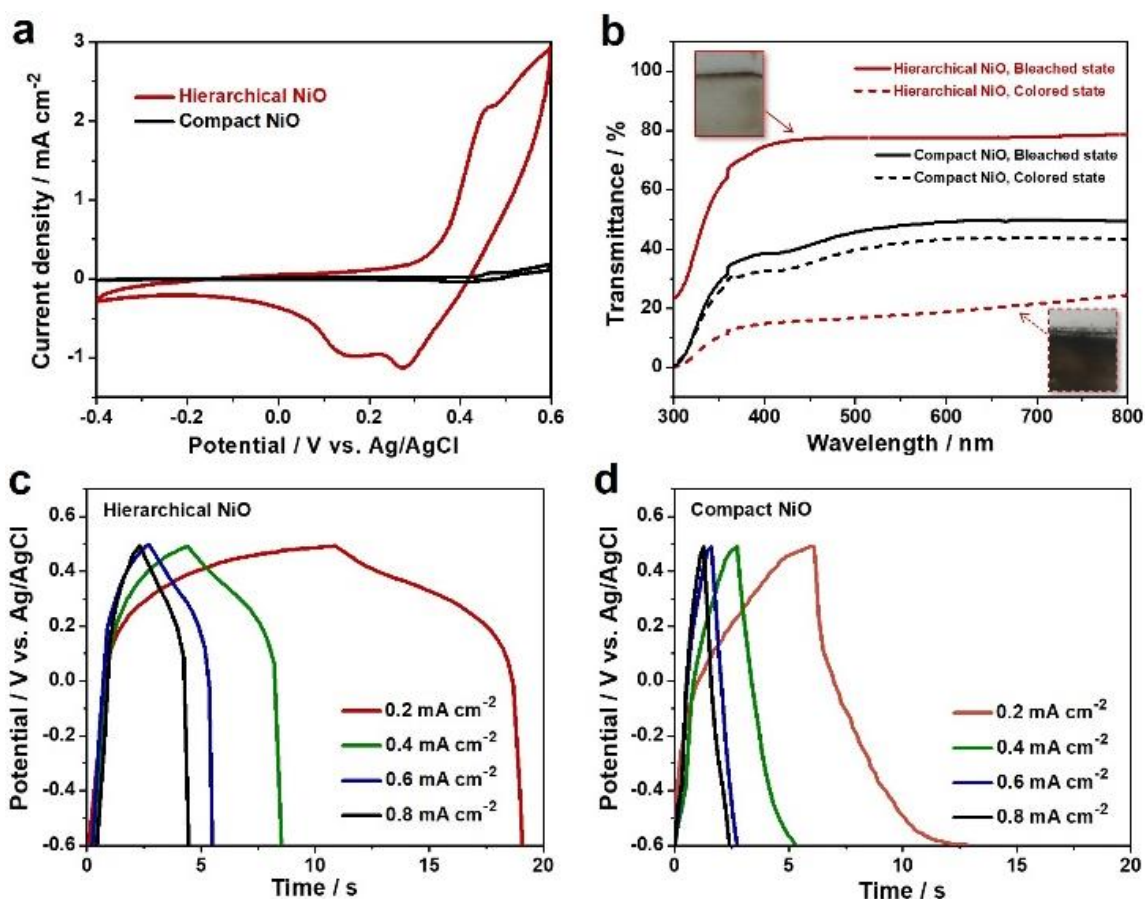


Figure 2. (a) Cyclic voltammetry properties of the hierarchical and compact NiO. (b) Transmittance spectra of hierarchical and compact NiO in the full bleached and colored states. Insets: Optical images of the hierarchical NiO at bleached and colored states. (c, d) Galvanostatic Charge/discharge curves of the hierarchical and compact NiO recorded at different current densities.

The electrolyte used here was KOH aqueous solution. As shown in Figure 3c, surface water contact angle of the compact NiO film was $38.2^\circ \pm 3^\circ$. When introducing a micro-nano hierarchical structure, the surface hydrophilicity was amplified because of a typical “locus leaf effect” [34]. Consequently, NiO film approached to a superhydrophilicity and the contact angle reduced to $\sim 10.5^\circ$ (Figure 3d). This facilitated ionic transport at the interface between electrolyte and NiO film as discussed above. Therefore, the construction of hierarchical structure contributed to a good electrical property, which in turn enhanced electrochromic and capacitive performances of NiO.

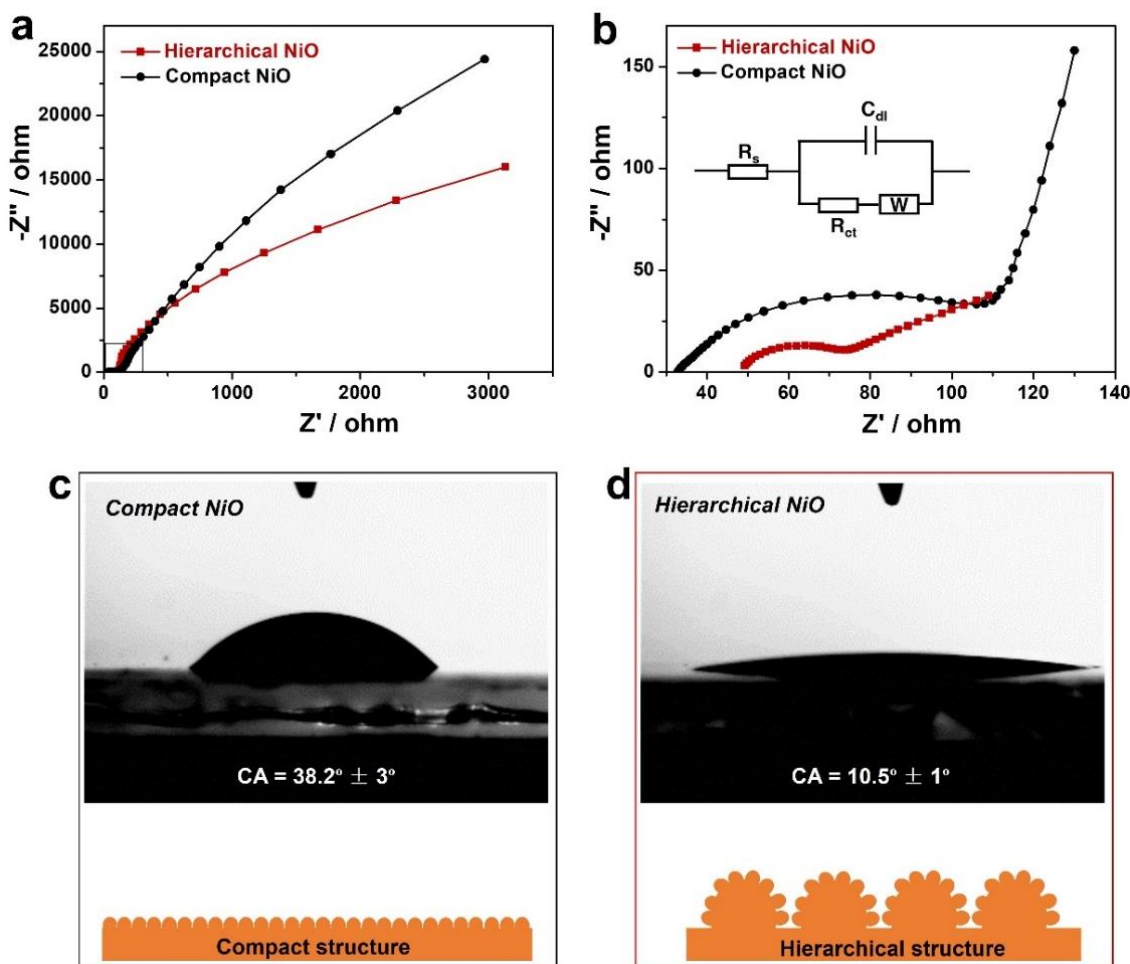


Figure 3. Nyquist curves (a) and the magnified ones in the high frequency region (b) of the EIS measurements for the two NiO film embedded electrodes. Surface water contact angle images and surface morphology schematic illustrations for hierarchical (c) and compact (d) NiO films.

4. CONCLUSIONS

In summary, NiO films with micro-nano hierarchical structure were prepared using a facile electrochemical deposition method and subsequent selective dissolution step. This hierarchical structure increased the specific surface area and amplified hydrophilicity of NiO film, which facilitated fast electron and ion transfer. Therefore, hierarchical NiO film embedded electrode demonstrated a superior electrochromic performance compared with traditional compact film. A high transparency modulation up to 64.5% could be obtained at 550 nm. Furthermore, the introduction of hierarchical structure enhanced the energy storage behavior of NiO. The capacitance of hierarchical NiO was 1.2 times larger than the compact one. This work provided a novel approach to fabricate micro-nano hierarchical structure for improving electrochemical performance of metal oxides.

ACKNOWLEDGEMENTS

This work was supported by National Key R&D Program of China (2016YFB0601700), National Natural Science Foundation of China (11804012, 21701003) and Beijing Natural Science Foundation (L182008, 4154090, 2161001).

References

1. A.L. Dyer, R. H. Bulloch, Y. Zhou, B. Kippelen, J. R. Reynolds and F. Zhang, *Adv. Mater.*, 26 (2014) 4895.
2. B.R. Koo, K.H. Kim, H.J. Ann, *Appl. Surf. Sci.*, 453 (2018) 238.
3. K. Siuzdak, M. Szkoda, M. Sawczak, J. Karczewski, J. Ryl and A. Cenian, *Thin Solid Films*, 659 (2018) 48.
4. C. Yan, W. Kang, J. Wang, M. Cui, X. Wang, C. Y. Foo, K. J. Chee and P. S. Lee, *ACS Nano*, 8 (2014) 316.
5. K. W. Silverstein, C. E. Halbig, J. S. Mehta, A. Sharma, S. Eigler and J. M. Mativetsky, *Nanoscale*, 11 (2019) 3112.
6. A.B. Kamaraj, H. Shrestha, E. Speck and M. Sundaram, *Procedia Manuf.*, 10 (2017) 478.
7. W. Chen, H. Yu, S. Y. Lee, T. Wei, J. Li and Z Fan, *Chem. Soc. Rev.*, 47 (2018) 2837.
8. J. H. Yu, H. Yang, R. H. Jung, J. W. Lee and J. H. Boo, *Thin Solid Films*, 664 (2018) 1.
9. Y. Chen, X. Li, Z. Bi, X He, G Li, X. Xu and X. Gao, *Appl. Surf. Sci.*, 440 (2018) 217.
10. M. Winter and R.J. Brodd, *Chem. Rev.*, 104 (2004) 4245.
11. S. Rima and M. Lattuada, *Small*, 14 (2018) 1802854.
12. M. S. Ambrosia and M. Y. Ha, *Comput. Fluids.*, 163 (2018) 1.
13. T. Darmanin, R. Bombera, P. Colpo, A. Valsesia, J. P. Laugier, F. Rossi and F. Guittard, *ChemPlusChem*. 82 (2017) 352.
14. Y. L. Lee and D. Morgan, *Phys. Rev. B: Condens. Matter Mater. Phys.*, 91 (2015) 195430
15. J. Li, W. Zhao, F. Huang, A. Manivannan and N. Wu, *Nanoscale*, 3 (2011) 5103.
16. Y. Lee, H. J. Choi, T. Kim, K. H. Hwang, J. H. Yu, S. H. Nam, D. H. Ryu and J. H. Boo, *Thin Solid Films*, 637 (2017) 14.
17. L. Zhao, G. Su, W. Liu, L. Cao, J Wang, Z. Dong and M. Song, *Appl. Surf. Sci.*, 257 (2011) 3974.
18. Y. Zhong, Z. Chai, Z. Liang, P. Sun, W. Xie, C. Zhao and W. Mai, *ACS Appl. Mater. Interfaces.*, 9 (2017) 34085.
19. K.K. Chiang and J. J. Wu, *ACS Appl. Mater. Interfaces.*, 5 (2013) 6502.
20. X. Wang, B. Liu, J. Tang, G. Dai, B. Dong, L. Cao, R. Gao and G. Su, *Sol. Energy Mater. Sol. Cells.*, 191 (2019) 108.
21. H. Yang, J. H. Yu, H.J. Seo, R. H. Jeong and J. H. Boo, *Appl. Surf. Sci.*, 461 (2018) 88.
22. D. Dong, W. Wang, A. Rougier, G. Dong, M. D. Rocha, L. Presmanes, K. Zrikem, G. Song, X. Diao and A. Barnabé, *Nanoscale*, 10 (35) (2018) 16521.
23. K. A. Lomachenkoab, C. Garino, E. Galloac, D. Gianoliod, R. Gobettoa, P. Glatzelc, N. Smolentsevb, G. Smolentseve, A. V. Soldatovb, C. Lambertia and Luca Salassaf, *Phys. Chem. Chem. Phys.*, 15 (2013) 16152.
24. Z. Yin and F. Chen, *Electrochim. Acta.*, 117 (2014) 84.
25. K. K. Purushothaman, S. J. Antony and G. Muralidharan, *Sol. Energy.*, 85 (2011) 978.
26. Y. E. Friat and A. Peksoz, *Electrochim. Acta.*, 295 (2019) 645.
27. G. A. Niklasson and C. G. Granqvist, *J. Mater. Chem.* 17 (2007) 127.
28. J. Guo, M. Wang, G. Dong, Z. Zhang, Q. Zhang, H. Yu, Y. Xiao, Q. Liu, J. Liu and X. Diao, *Inorg. Chem.*, 57 (2018) 8874.
29. K. K. Purushothaman and G. Muralidharan, *Mater. Sci. Semicond. Process.*, 14 (2011) 78.
30. Y. Chen, Y. Wang, P. Sun, *J. Mater. Chem. A.*, 3 (2015) 20614.

31. L Zhu, C. K. N. Peh, T. Zhu, Y. F. Lim and G. W. Ho, *J. Mater. Chem. A*, 5 (2017) 8343.
32. X. Wei, S. Wan and S. Gao, *Nano Energy*, 28 (2016) 206.
33. Y. Chen, X. Li, Z. Bi, X. He, G. Li, X. Xu and X. Gao, *Appl. Surf. Sci.*, 440 (2018) 217.
34. X. Li, J. Wang, Y. Zhao and X. Zhang, *ACS Appl. Mater. Interfaces.*, 10 (2018) 16901.

© 2019 The Authors. Published by ESG (www.electrochemsci.org). This article is an open access article distributed under the terms and conditions of the Creative Commons Attribution license (<http://creativecommons.org/licenses/by/4.0/>).